The proton structure in the LHC era

Sven-Olaf Moch

Universität Hamburg

Universität Hamburg
DER FORSCHUNG | DER LEHRE | DER BILDUNG

European Research Council
Established by the European Commission

Motivation

Standard Model cross sections

- Standard Model cross sections and predictions at the LHC CMS coll. ‘22

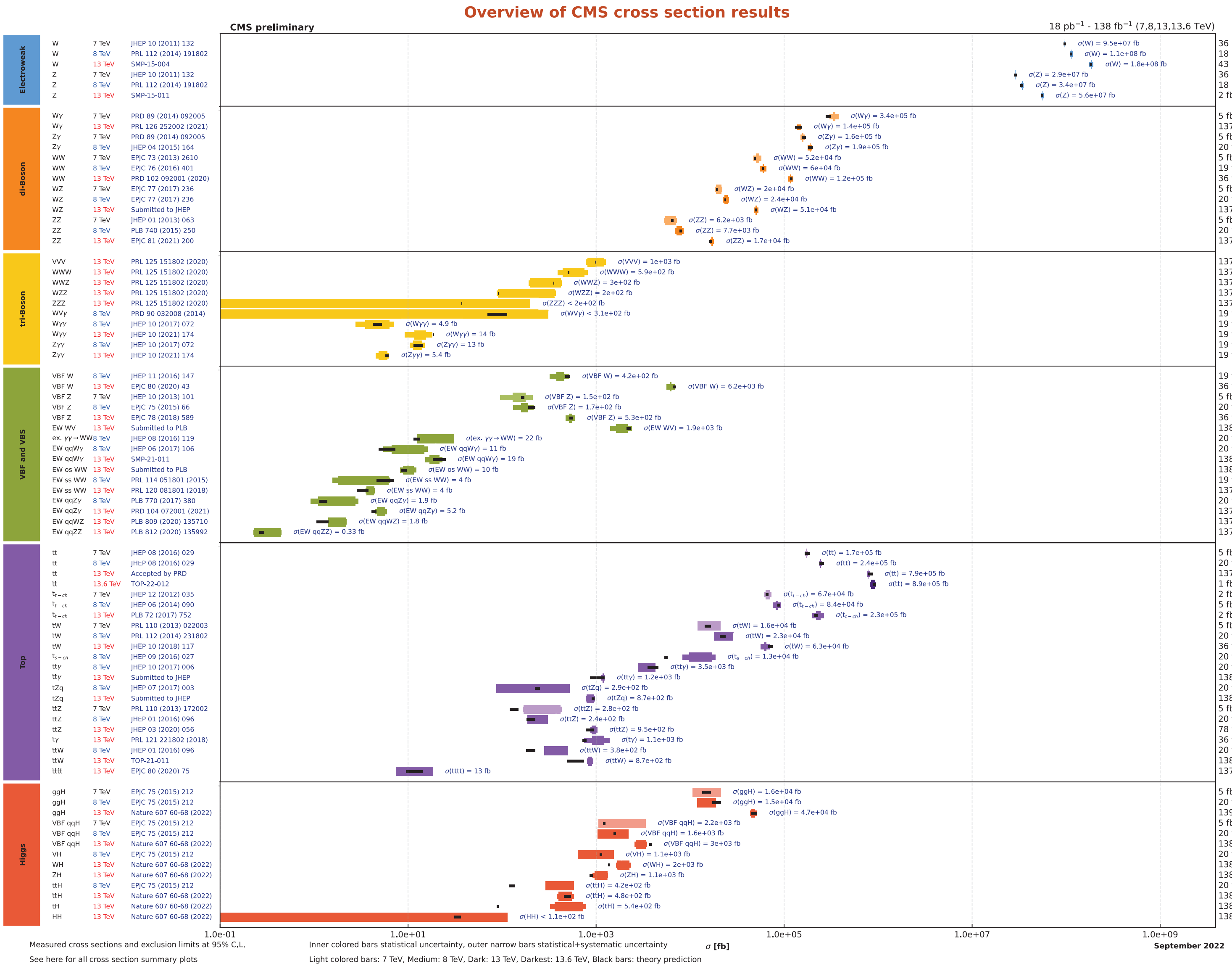

QCD factorization

QCD factorization

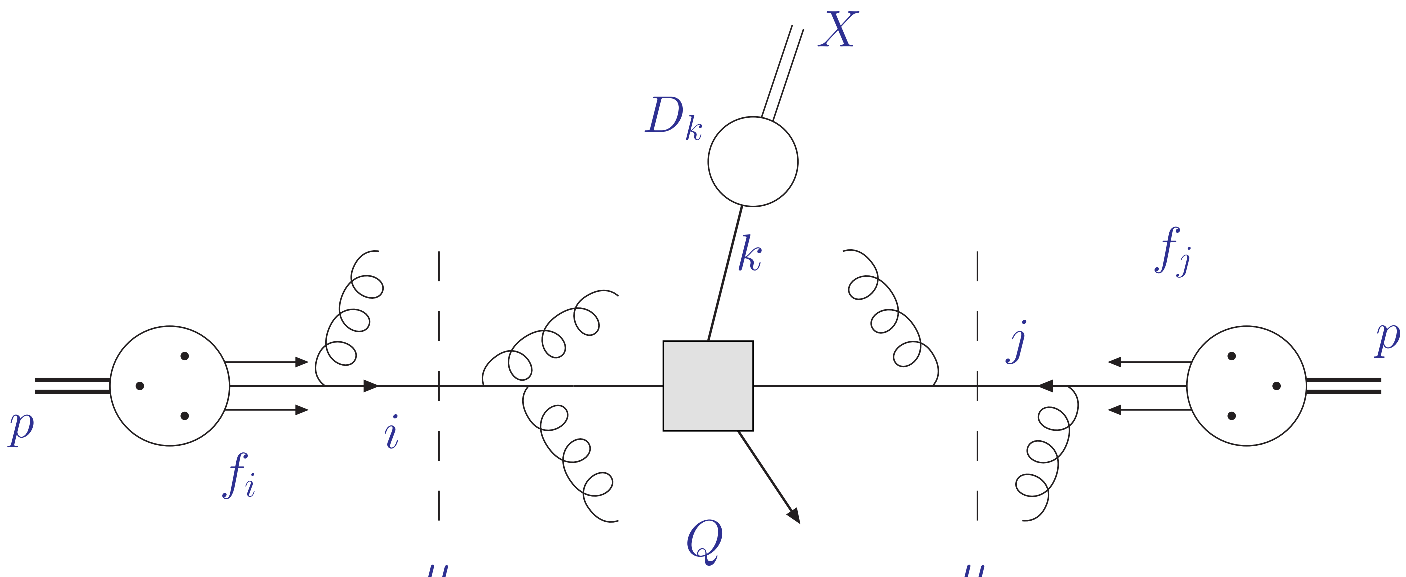

$$\sigma_{pp\to X} = \sum_{ij} f_i(\mu^2) \otimes f_j(\mu^2) \otimes \hat{\sigma}_{ij\to X}\left(\alpha_s(\mu^2), Q^2, \mu^2, m_X^2\right)$$

- Factorization at scale μ
  - separation of sensitivity to dynamics from long and short distances
- Hard parton cross section $\hat{\sigma}_{ij\to X}$ calculable in perturbation theory
  - cross section $\hat{\sigma}_{ij\to k}$ for parton types i, j and hadronic final state X
- Non-perturbative parameters: parton distribution functions f_i, strong coupling α_s, particle masses m_X
  - known from global fits to exp. data, lattice computations, ...

Hard scattering cross section

- Parton cross section $\hat{\sigma}_{ij\to k}$ calculable pertubatively in powers of α_s
  - known to NLO, NNLO, ... ($\mathcal{O}(\text{few}\%)$ theory uncertainty)

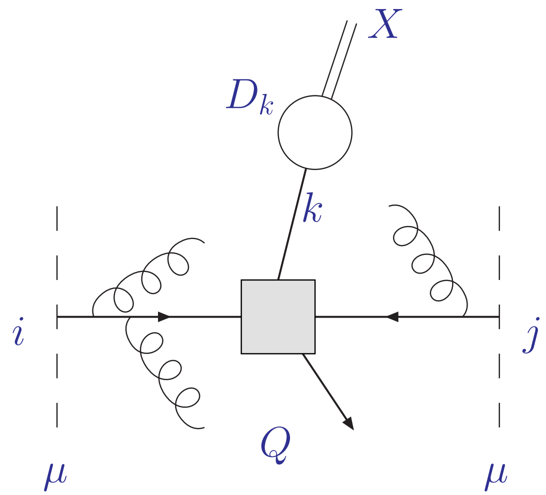

- Accuracy of perturbative predictions
  - LO (leading order) ($\mathcal{O}(50-100\%)$ unc.)
  - NLO (next-to-leading order) ($\mathcal{O}(10-30\%)$ unc.)
  - NNLO (next-to-next-to-leading order) ($\lesssim$ $\mathcal{O}(10\%)$ unc.)
  - N^3LO (next-to-next-to-next-to-leading order)
  - ...

Parton luminosity

- Long distance dynamics due to proton structure

- Cross section depends on parton distributions f_i

$$\sigma_{pp\to X} = \sum_{ij} f_i(\mu^2) \otimes f_j(\mu^2) \otimes \left[\ldots\right]$$

- Parton distributions known from global fits to exp. data
  - available fits accurate to NNLO
  - information on proton structure depends on kinematic coverage

Deep-inelastic scattering

Classic example

- Deep-inelastic scattering
  - test parton dynamics at factorization scale μ

$$\sigma_{\gamma p \to X} = \sum_i f_i(\mu^2) \otimes \hat{\sigma}_{\gamma i \to X} \left(\alpha_s(\mu^2), Q^2, \mu^2\right)$$

Physics picture

- QCD factorization
  - constituent partons from proton interact at short distance
  - photon momentum $Q^2 = -q^2$, Bjorken's $x = Q^2/(2p \cdot q)$
  - low resolution

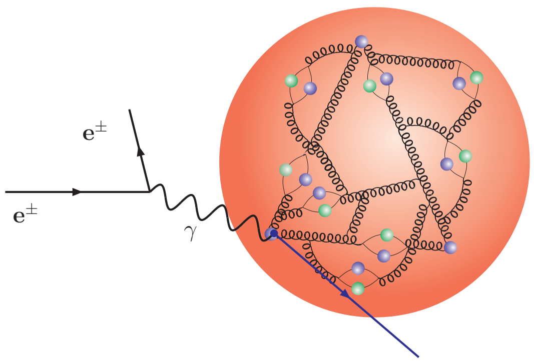

high resolution

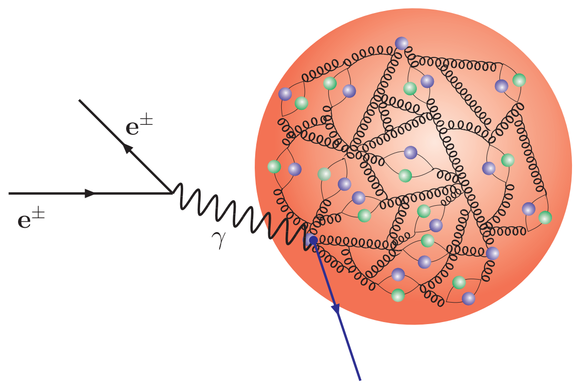

Once upon a time ...

- HERA: deep structure of proton at highest Q^2 and smallest x

Bright future for precision hadron physics

- Electron-Ion Collider
  A machine that will unlock the secrets of the strongest force in Nature

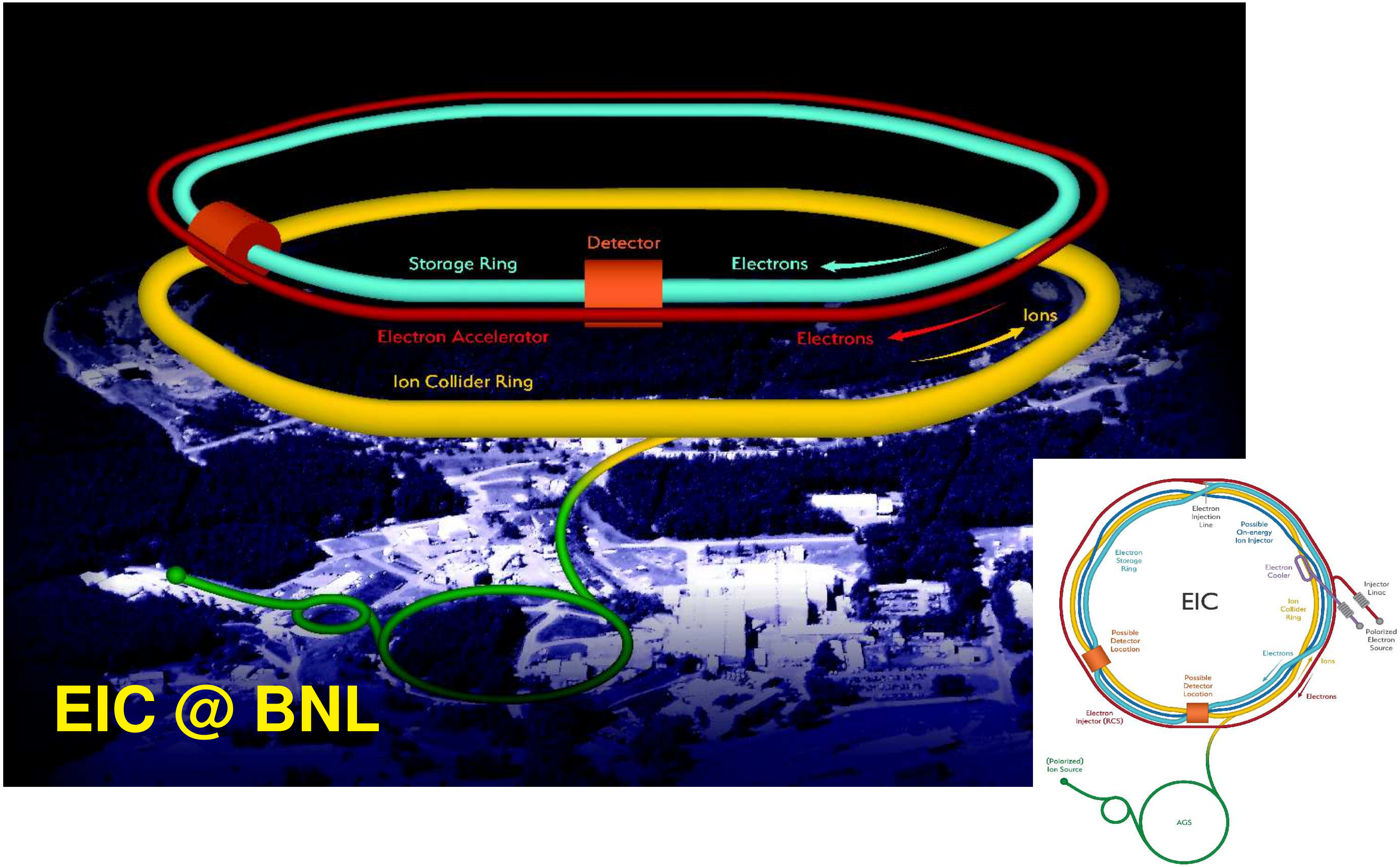

Inelastic electron-proton scattering

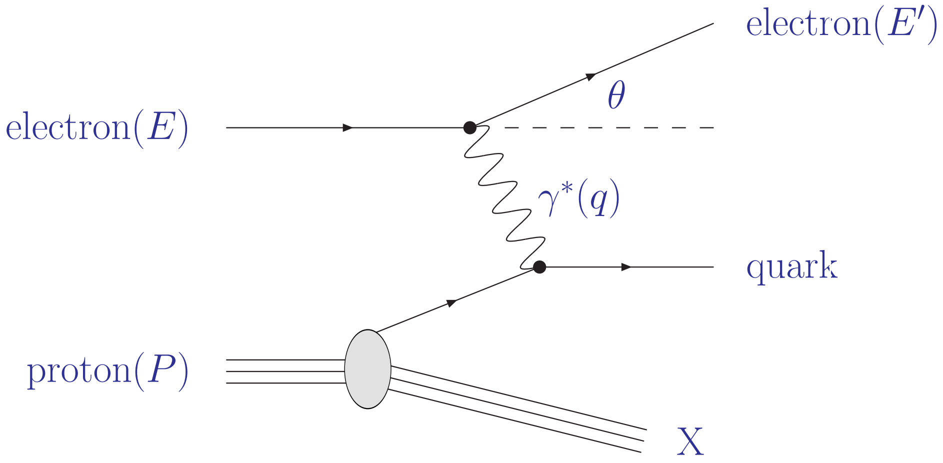

- Virtuality of photon: resolution
  $$Q^2 \equiv -q^2 = 4EE' \sin^2(\theta/2)$$

- Bjorken variable: inelasticity
  $$x = \frac{Q^2}{2P\cdot q} < 1$$

- Cross section (X inclusive): proton structure function F_i^p

$$(E - E')\frac{d\sigma}{d\Omega\, dE'} \overset{\text{lab}}{=} \underbrace{\frac{\alpha^2 \cos^2\frac{\theta}{2}}{4E^2 \sin^4\frac{\theta}{2}}}_{\text{Mott-scattering (point-like)}} \left\{ F_2^p(x, Q^2) + \tan^2\frac{\theta}{2}\, F_1^p(x, Q^2) \right\}$$

Inelastic electron-proton scattering

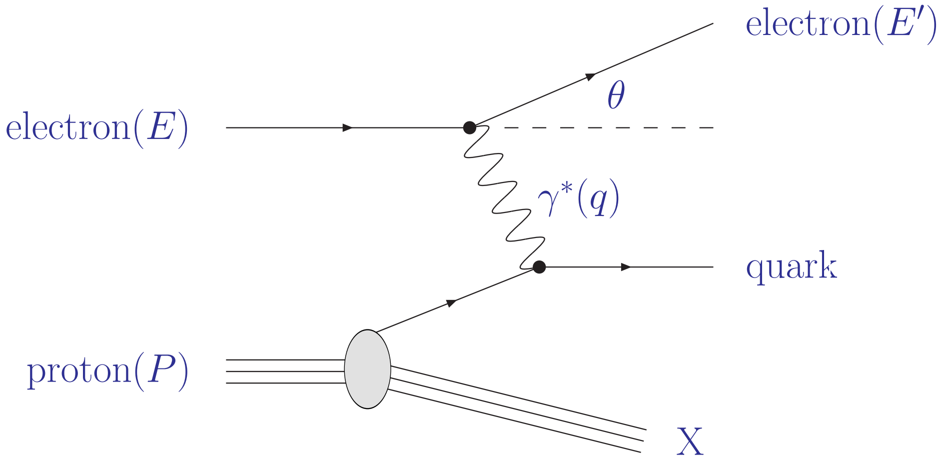

- Virtuality of photon: resolution
  $$Q^2 \equiv -q^2 = 4EE' \sin^2(\theta/2)$$

- Bjorken variable: inelasticity
  $$x = \frac{Q^2}{2P\cdot q} < 1$$

- Cross section (X inclusive): proton structure function F_i^p

$$(E - E')\frac{d\sigma}{d\Omega\, dE'} \overset{\text{lab}}{=} \underbrace{\frac{\alpha^2 \cos^2 \frac{\theta}{2}}{4E^2 \sin^4 \frac{\theta}{2}}}_{\text{Mott-scattering (point-like)}} \left\{ F_2^p(x, Q^2) + \tan^2 \frac{\theta}{2}\, F_1^p(x, Q^2) \right\}$$

- Deep-inelastic scattering (Bjorken limit: $Q^2 \to \infty$ and x fixed)
  Parton modell (quasi-free point-like constituents, incoherence)
  $$F_2(x, Q^2) \simeq F_2(x) = \sum_i e_i^2\, x f_i(x)$$
  - $x f_i(x)$ distribution for momentum fraction x of parton i

Deep-inelastic scattering

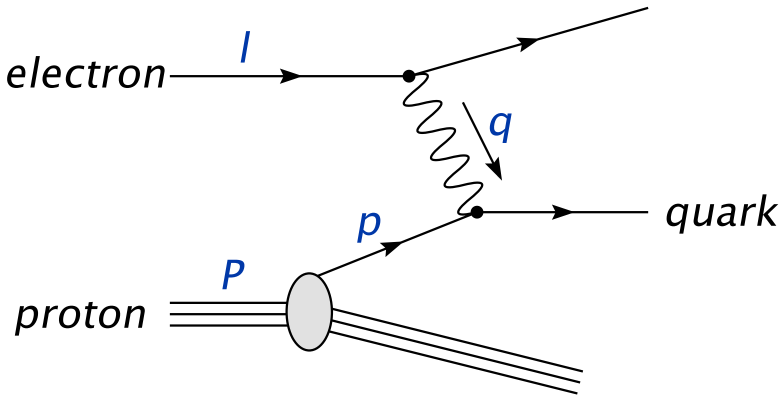

Kinematic variables

- momentum transfer $Q^2 = -q^2$
- Bjorken variable $x = Q^2/(2p \cdot q)$

- Structure function F_2^p (up to order $\mathcal{O}(1/Q^2)$)

$$x^{-1} F_2^p(x, Q^2) \;=\; \sum_i \int_x^1 \frac{d\xi}{\xi}\, C_{2,i}\left(\frac{x}{\xi}, \alpha_s(\mu^2), \frac{\mu^2}{Q^2}\right) f_i^p(\xi, \mu^2)$$

- Coefficient functions

$$C_{a,i} = \alpha_s^n \left(c_{a,i}^{(0)} + \alpha_s c_{a,i}^{(1)} + \alpha_s^2 c_{a,i}^{(2)} + \alpha_s^3 c_{a,i}^{(3)} + \alpha_s^4 c_{a,i}^{(4)} + \dots \right)$$

  - current frontier in perturbation theory $\mathrm{N^4LO}$ (work in progress)

Parton evolution

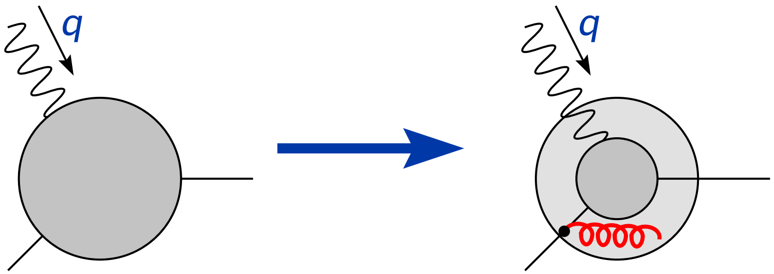

- Feynman diagrams in leading order

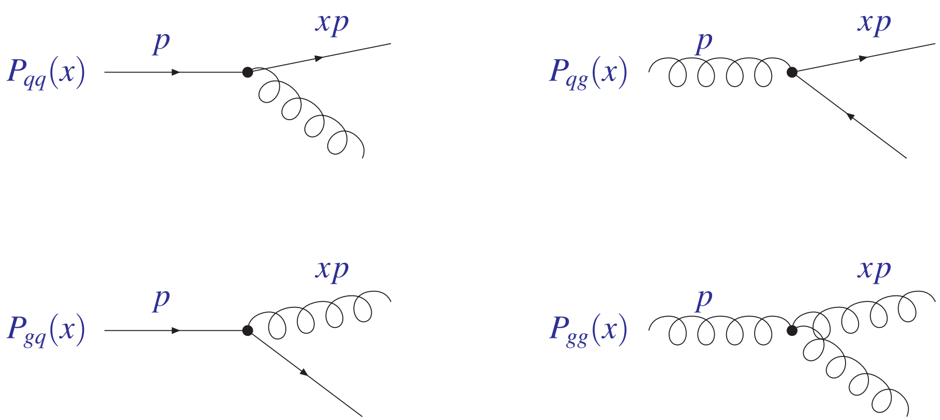

- Proton in resolution $1/Q \longrightarrow$ sensitive to lower momentum partons

- Evolution equations for parton distributions f_i
  - predictions from fits to reference processes (universality)

$$\frac{d}{d\ln\mu^2} f_i(x,\mu^2) \;=\; \sum_k \left[P_{ik}(\alpha_s(\mu^2)) \otimes f_k(\mu^2)\right](x)$$

- Splitting functions P up to N^{3}LO (work in progress)

$$P \;=\; \underbrace{\alpha_s\, P^{(0)} \;+\; \alpha_s^2\, P^{(1)} \;+\; \alpha_s^3\, P^{(2)}}_{\text{NNLO: standard approximation}} + \alpha_s^4\, P^{(3)} + \ldots$$

Parton distributions in proton

- Valence $q - \bar{q}$ (additive quantum numbers) sea (part with $q + \bar{q}$)

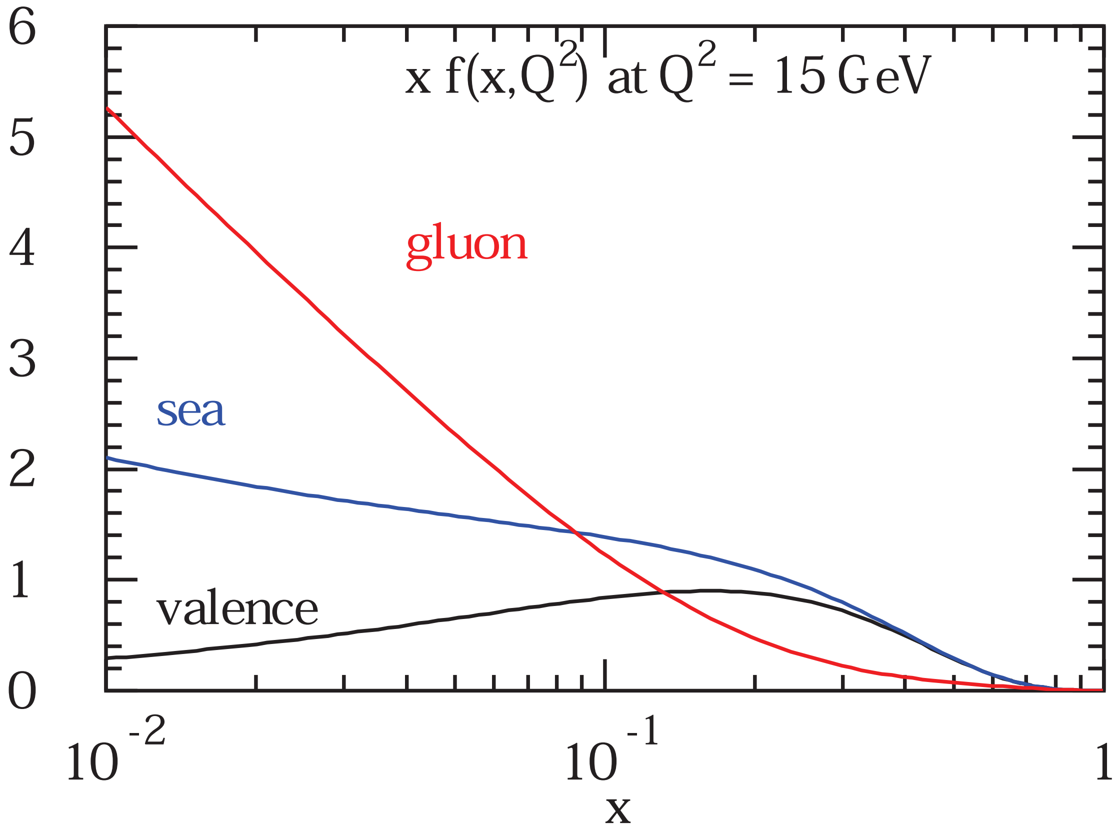

- Parameterization (bulk of data from deep-inelastic scattering)
  - structure function $F_2 \longrightarrow$ quark distribution
  - scale evolution (perturbative QCD) $\longrightarrow$ gluon distribution

Parton distributions in proton

- Valence $q - \bar{q}$ (additive quantum numbers) sea (part with $q + \bar{q}$)

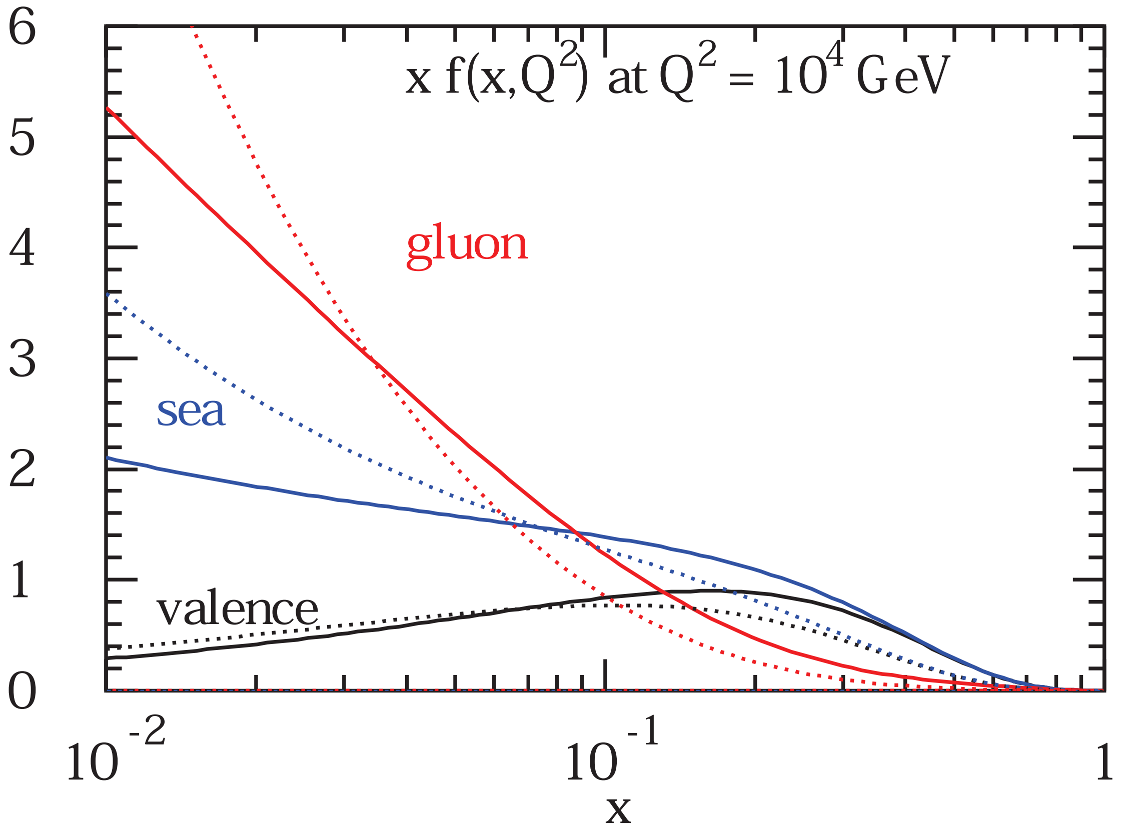

- Parameterization (bulk of data from deep-inelastic scattering)
  - structure function $F_2 \longrightarrow$ quark distribution
  - scale evolution (perturbative QCD) $\longrightarrow$ gluon distribution

Parton content of the proton

The LHC

- Highest energies at colliders until 203x

Parton kinematics at LHC

- Information on proton structure depends on kinematic coverage

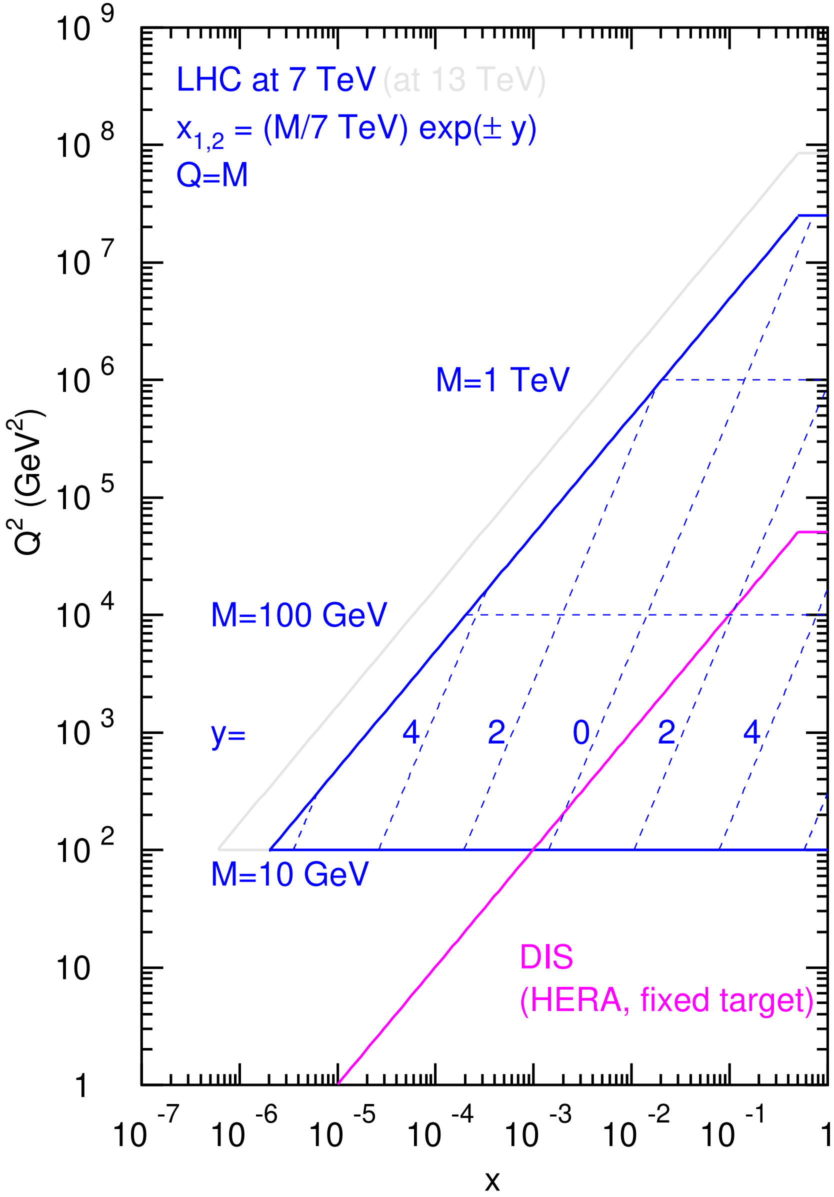

- LHC run at $\sqrt{s}$ = 7/8 TeV ($\sqrt{s}$ = 13 TeV)
  - parton kinematics well covered by HERA and fixed target experiments
- Parton kinematics with $x_{1,2} = M/\sqrt{S}\mathrm{e}^{\pm y}$
  - forward rapidities sensitive to small-x
- Cross section depends on convolution of parton distributions
  - small-x part of f_i and large-x PDFs f_j

$$\sigma_{pp\to X} = \sum_{ij} f_i(\mu^2) \otimes f_j(\mu^2) \otimes \Big[\ldots\Big]$$

Data in global PDF fits (I)

Data sets considered in ABMP16 analysis

Alekhin, Blümlein, S.M., Placakyte '17

- Analysis of world data for deep-inelastic scattering, fixed-target data for Drell-Yan process and collider data ($W^{\pm}$-, Z-bosons, top-quarks)
  - inclusive DIS data HERA, BCDMS, NMC, SLAC ($NDP = 2155$)
  - semi-inclusive DIS charm-, bottom-quark data HERA ($NDP = 81$)
  - Drell-Yan data (fixed target) E-605, E-866 ($NDP = 158$)
  - neutrino-nucleon DIS (di-muon data) CCFR/NuTeV, CHORUS, NOMAD ($NDP = 232$)
  - $W^{\pm}$-, Z-boson production data D0, ATLAS, CMS, LHCb ($NDP = 172$)
  - inclusive top-quark hadro-production CDF&D0, ATLAS, CMS ($NDP = 24$)

Iterative cycle of PDF fits

i) check of compatibility of new data set with available world data

ii) study of potential constraints due to addition of new data set to fit

iii) perform high precision measurement of PDFs, strong coupling $\alpha_s(M_Z)$ and heavy quark masses m_c, m_b, m_t,

ABMP16 PDF ansatz

- PDFs parameterization at scale $\mu_0 = 3\text{GeV}$ in scheme with $n_f = 3$

  Alekhin, Blümlein, S.M., Placakyte '17

  - ansatz for valence-/sea-quarks, gluon

$$
\begin{aligned}
xq_v(x,\mu_0^2) &= \frac{2\delta_{qu} + \delta_{qd}}{N_q^v} x^{a_q} (1-x)^{b_q} x^{P_{qv}(x)} \\
xq_s(x,\mu_0^2) &= x\bar{q}_s(x,\mu_0^2) = A_{qs} (1-x)^{b_{qs}} x^{a_{qs} P_{qs}(x)} \\
xg(x,\mu_0^2) &= A_g x^{a_g} (1-x)^{b_g} x^{a_g P_g(x)}
\end{aligned}
$$

  - strange quark is taken in charge-symmetric form
  - function $P_p(x) = (1 + \gamma_{-1,p} \ln x) \left(1 + \gamma_{1,p} x + \gamma_{2,p} x^2 + \gamma_{3,p} x^3\right)$,
  - 29 parameters in fit including $\alpha_s^{(n_f=3)}(\mu_0 = 3$ GeV), m_c, m_b and m_t
  - simultaneous fit of higher twist parameters (twist-4)
- Ansatz provides sufficient flexibility; no additional terms required to improve the quality of fit
- Large x part of all PDFs $\sim (1-x)^b$, where $b_{u_v} = 3.443 \pm 0.064$, $b_{d_v} = 4.47 \pm 0.55$, $b_{u_s} = 7.75 \pm 0.39$, $b_{d_s} = 8.41 \pm 0.34$, ...

Top-quark hadro-production

Top-quark hadro-production cross section

- Cross section for $t\bar{t}$-production with parametric dependence

$$\sigma_{pp\to X} \quad = \quad \sum_{ij} f_i(\mu^2) \otimes f_j(\mu^2) \otimes \underbrace{\hat{\sigma}_{ij\to X}\left(\alpha_s(\mu^2), Q^2, \mu^2, m_X^2\right)}$$

$$= \hat{\sigma}^{(0)}_{ij\to X} + \alpha_s\, \hat{\sigma}^{(1)}_{ij\to X} + \alpha_s^2\, \hat{\sigma}^{(2)}_{ij\to X} + \dots$$

  - PDFs f_i, strong coupling α_s, masses m_X
- Correlation of PDFs, $\alpha_s(M_Z)$ and m_t in global fit
  - effective parton $\langle x\rangle \sim 2m_t/\sqrt{s} \sim 2.5\dots 5\cdot 10^{-2}$

Top-quark mass determination

- Choice of renormalization scheme for treatment of heavy quarks
  - heavy quark mass in on-shell scheme $m_t^{\rm pole}$
  - running quark mass in $\overline{\rm MS}$-scheme $m_t(\mu)$
- Intrinsic limitation of sensitivity in total cross section

$$\left|\frac{\Delta\sigma_{t\bar{t}}}{\sigma_{t\bar{t}}}\right| \simeq 5\times\left|\frac{\Delta m_t}{m_t}\right|$$

Data on top-quark cross sections (2023)

experiment	decay channel	dataset	luminosity	$\sqrt{s}$	ref.
ATLAS & CMS	combined	2011	5 fb^{-1}	7 TeV	2205.13830
ATLAS & CMS	combined	2012	20 fb^{-1}	8 TeV	2205.13830
ATLAS	dileptonic, semileptonic	2011	257 pb^{-1}	5.02 TeV	2207.01354
CMS	dileptonic	2011	302 pb^{-1}	5.02 TeV	2112.09114
ATLAS	dileptonic	2015-2018	140 fb^{-1}	13 TeV	2303.15340
ATLAS	semileptonic	2015-2018	139 fb^{-1}	13 TeV	2006.13076
CMS	dileptonic	2016	35.9 fb^{-1}	13 TeV	1812.10505
CMS	semileptonic	2016-2018	137 fb^{-1}	13 TeV	2108.02803
ATLAS	dileptonic	2022	11.3 fb^{-1}	13.6 TeV	ATLAS-CONF-2023-006
CMS	dileptonic, semileptonic	2022	1.21 fb^{-1}	13.6 TeV	2303.10680

Experiment	decay channel	dataset	luminosity	$\sqrt{s}$	observable(s)	n	ref.
CMS	semileptonic	2016–2018	137 fb^{-1}	13 TeV	$M(t\bar{t})$, $\lvert y(t\bar{t})\rvert$	34	2108.02803
CMS	dileptonic	2016	35.9 fb^{-1}	13 TeV	$M(t\bar{t})$, $\lvert y(t\bar{t})\rvert$	15	1904.05237
ATLAS	semileptonic	2015–2016	36 fb^{-1}	13 TeV	$M(t\bar{t})$, $\lvert y(t\bar{t})\rvert$	19	1908.07305
ATLAS	all-hadronic	2015–2016	36.1 fb^{-1}	13 TeV	$M(t\bar{t})$, $\lvert y(t\bar{t})\rvert$	10	2006.09274
CMS	dileptonic	2012	19.7 fb^{-1}	8 TeV	$M(t\bar{t})$, $\lvert y(t\bar{t})\rvert$	15	1703.01630
ATLAS	semileptonic	2012	20.3 fb^{-1}	8 TeV	$M(t\bar{t})$	6	1511.04716
ATLAS	dileptonic	2012	20.2 fb^{-1}	8 TeV	$M(t\bar{t})$	5	1607.07281
ATLAS	dileptonic	2011	4.6 fb^{-1}	7 TeV	$M(t\bar{t})$	4	1607.07281
ATLAS	semileptonic	2011	4.6 fb^{-1}	7 TeV	$M(t\bar{t})$	4	1407.0371

- Measurements of top-quark hadro-production ATLAS, CMS
  - total inclusive $t\bar{t} + X$ cross sections ($NDP = 10$)
  - differential $t\bar{t} + X$ cross sections in $M(t\bar{t})$, $y(t\bar{t})$ ($NDP = 112$)

Theory status 2023

- NNLO QCD differential predictions for top-quark pairs at the LHC
  Czakon, Heymes, Mitov ‘15
- Top-quark pair hadroproduction at NNLO in QCD
  Catani, Devoto, Grazzini, Kallweit, Mazzitelli, Sargsyan ‘19
  - to be implemented in future public release of MATRIX code
    Catani, Devoto, Grazzini, Kallweit, Mazzitelli ‘19
- NNLO event generation for top-quark pair production
  Mazzitelli, Monni, Nason, Re, Wiesemann and Zanderighi ‘20
- Top-pair production at the LHC with MiNNLO_PS
  Mazzitelli, Monni, Nason, Re, Wiesemann and Zanderighi ‘21
- Narrow-width-approximation at NNLO
  - NNLO QCD corrections to leptonic observables in top-quark pair production and decay
    - implemented in private STRIPPER code
      Czakon, Mitov, Poncelet ‘20

Differential cross sections (I)

Challenges

- NNLO codes not easily publicly usable/accessible
- Very long run times (few CPU years) for distributions with fixed input parameters (m_t, PDFs, . . .)
- Accuracy of NNLO subtraction schemes
  - local sector subtraction (STRIPPER)
  - phase space slicing with q_T^{cut} (MATRIX)

Needs

- NNLO QCD predictions for range of m_t values
- Variation of PDFs (complete set of eigenvectors)

Solution

- Customized version of MATRIX — Garzelli, Mazzitelli, SM, Zenaiev '23
  - interface to PineAPPL library for storage of grids

Differential cross sections (II)

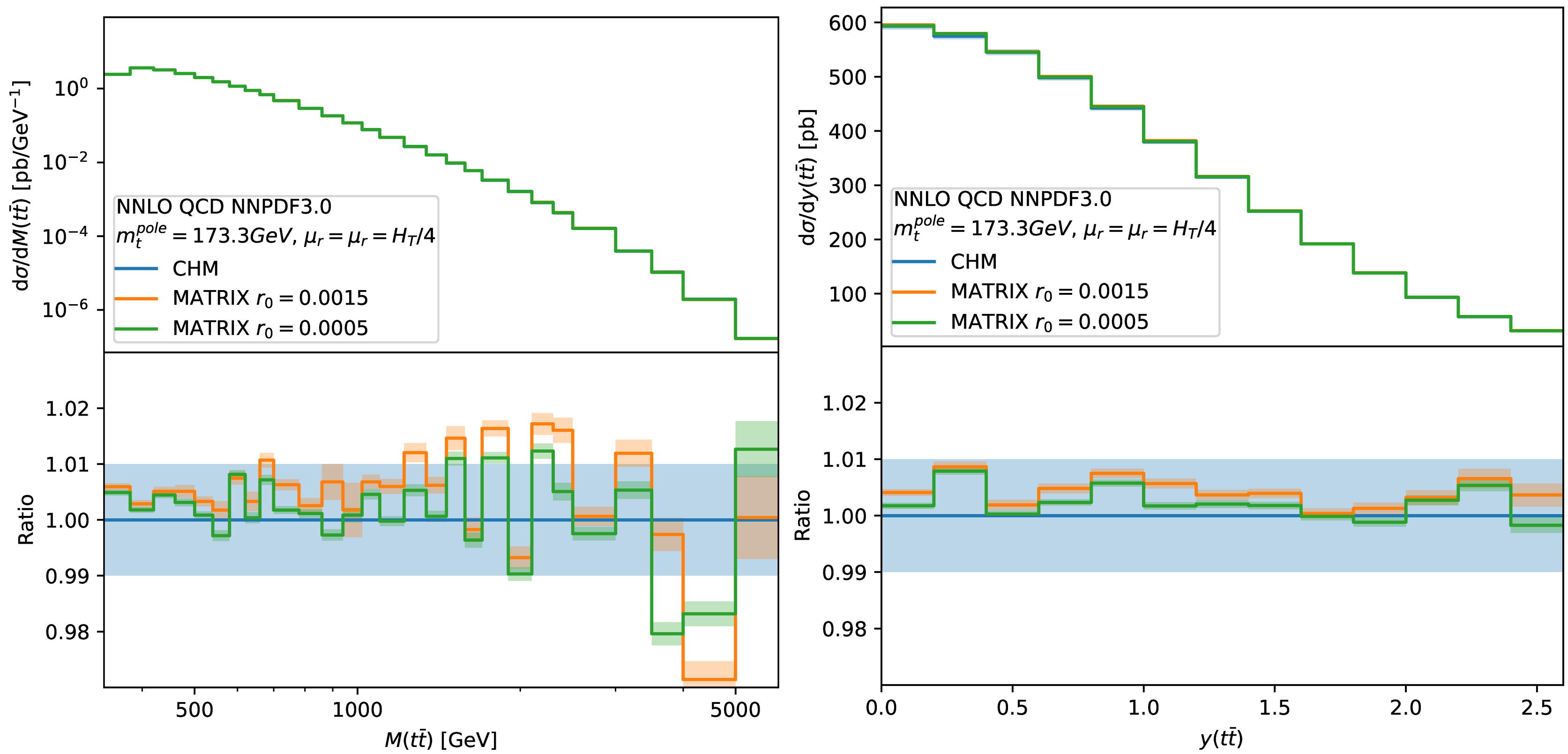

- Validation of MATRIX using cuts $r_0 = 0.0015$ and $r_0 = 0.0005$ with results from Czakon, Heymes, Mitov '17 with their numerical uncertainties
- NNLO differential cross sections — Garzelli, Mazzitelli, SM, Zenaiev '23
  - left: for invariant mass of $t\bar{t}$-pair
  - riht: the rapidity of $t\bar{t}$-pair

Differential cross sections (III)

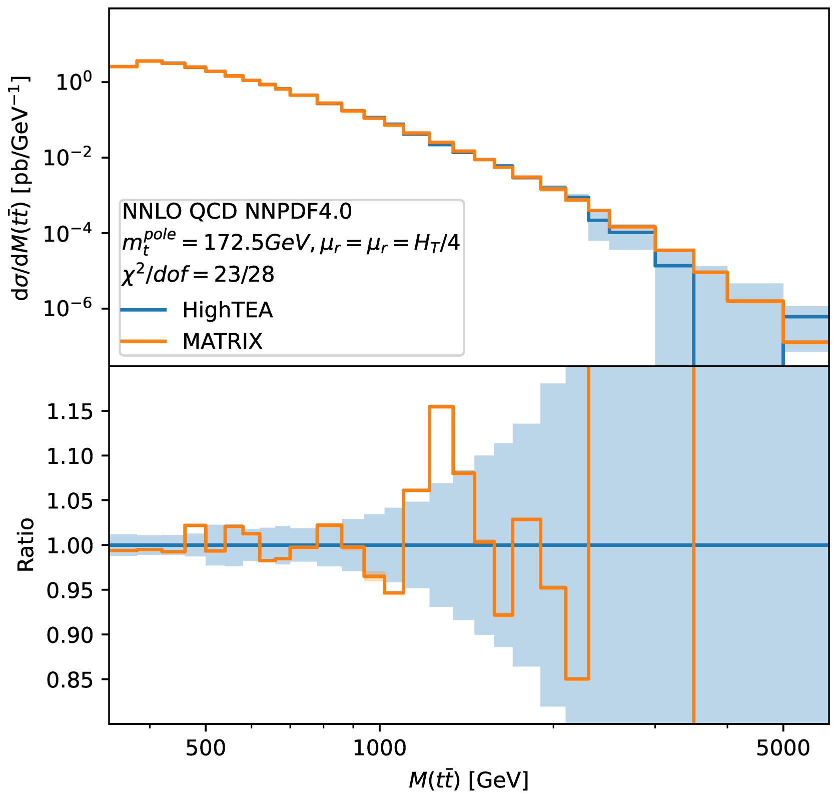

- Validation of MATRIX results for $M(t\bar{t})$ distribution with HighTEA project Czakon, Kassabov, Mitov, Poncelet, Popescu '23.
  - error bars account for numerical uncertainties in computations Garzelli, Mazzitelli, SM, Zenaiev '23

Top-quark data comparision (I)

Garzelli, Mazzitelli, SM, Zenaiev '23

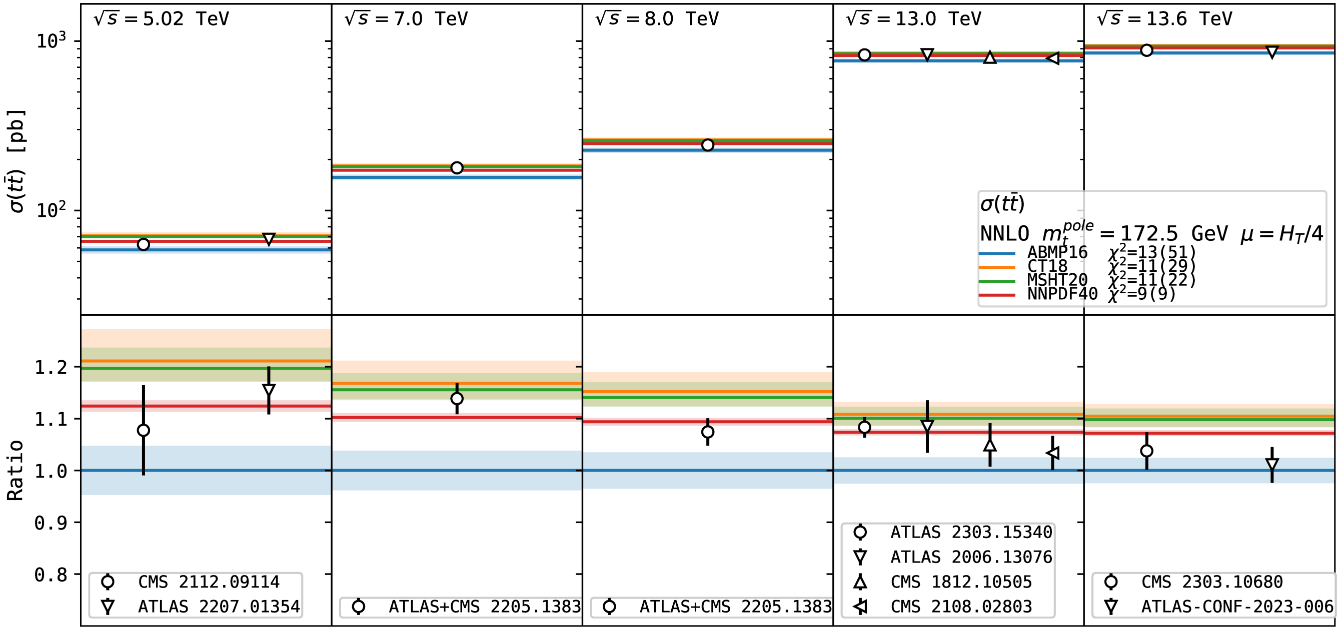

- Experimental data on total $t\bar{t} + X$ cross sections at different $\sqrt{s}$ ATLAS, CMS
  - comparision to NNLO predictions ($m_t^{\rm pole} = 172.5$ GeV)
  - different PDF sets ABMP16, CT18, MHST20, NNPDF4.0

Top-quark data comparision (II)

Garzelli, Mazzitelli, SM, Zenaiev '23

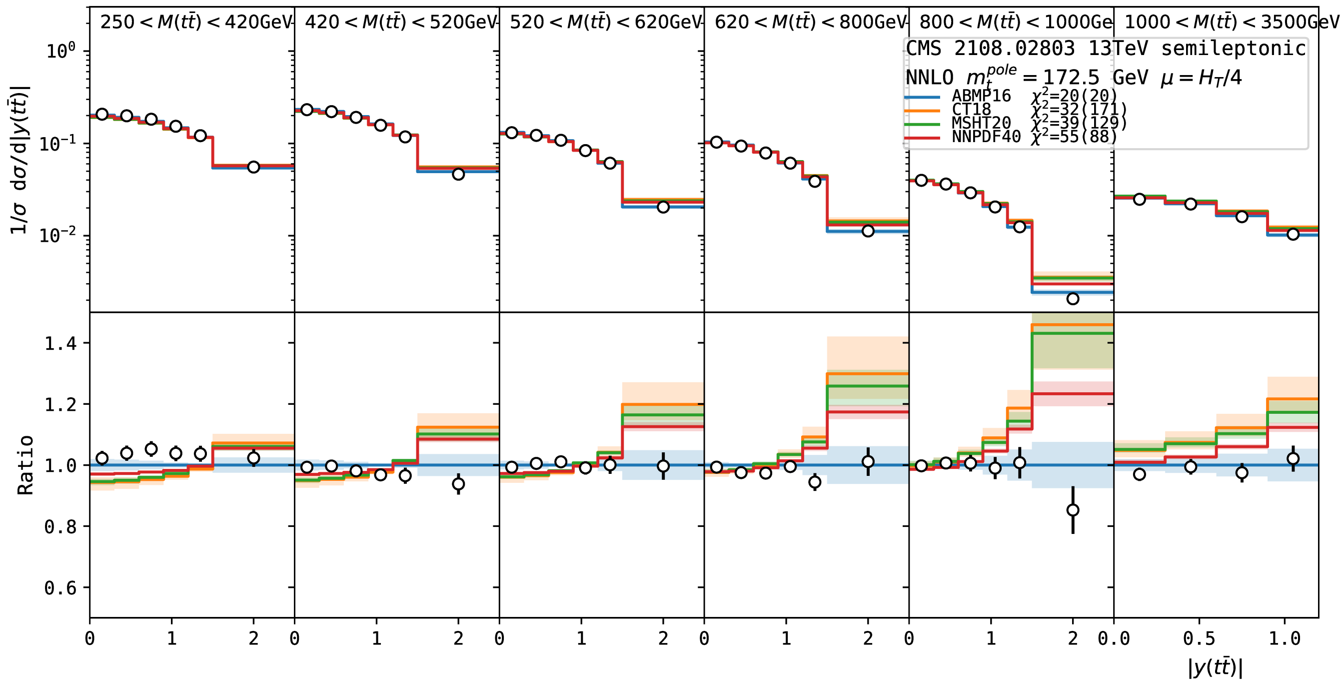

Semi-leptonic decay

- Experimental data on $t\bar{t} + X$ cross sections differential in $y(t\bar{t})$ CMS
  - comparision to NNLO predictions ($m_t^{\text{pole}} = 172.5$ GeV)
  - different PDF sets ABMP16, CT18, MHST20, NNPDF4.0

Top-quark data comparision (III)

Garzelli, Mazzitelli, SM, Zenaiev '23

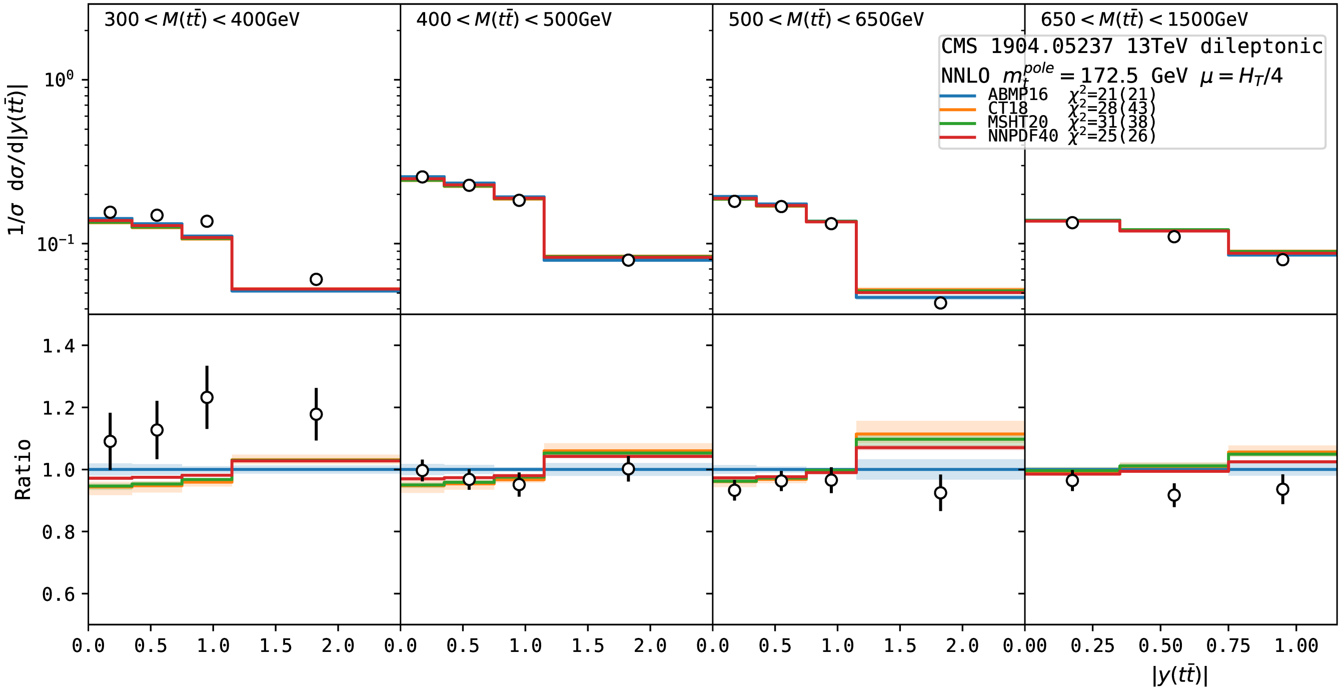

Di-leptonic decay

- Experimental data on $t\bar{t} + X$ cross sections differential in $y(t\bar{t})$ CMS
  - comparision to NNLO predictions ($m_t^{\rm pole} = 172.5$ GeV)
  - different PDF sets ABMP16, CT18, MHST20, NNPDF4.0

Top-quark mass determination (I)

Garzelli, Mazzitelli, SM, Zenaiev ‘23

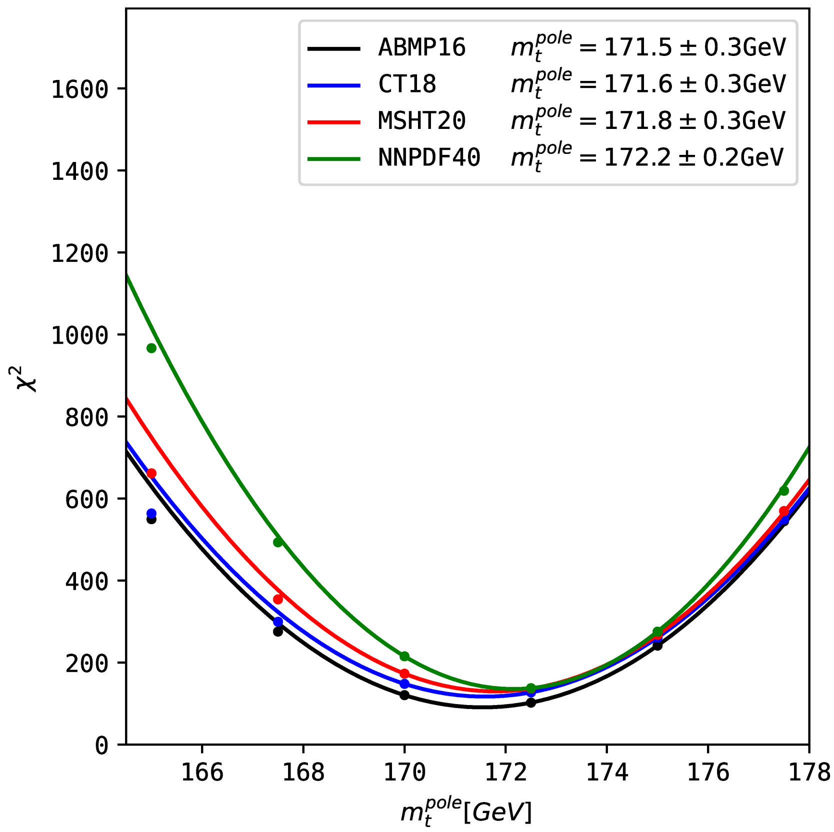

- Extraction of $m_t^{\rm pole}$ at NNLO from all experimental data
  - different PDF sets ABMP16, CT18, MHST20, NNPDF4.0
- Goodness-of-fit estimator χ^2 for extracted $m_t^{\rm pole}$ values

Fit quality

Data set	n	ABMP16	CT18	MSHT20	NNPDF4.0
CMS 13 TeV semileptonic 2108.02803	34	19(20)	29(176)	38(132)	55(90)
CMS 13 TeV dileptonic 1904.05237	15	15(15)	23(38)	27(34)	23(23)
ATLAS13 TeV semileptonic 1908.07305	19	11(15)	12(17)	11(13)	12(12)
ATLAS 13 TeV all-hadronic 2006.09274	10	11(11)	16(19)	16(17)	14(14)
CMS 8 TeV dileptonic 1703.01630	15	11(15)	11(12)	11(12)	12(12)
ATLAS 8 TeV semileptonic 1511.04716	6	10(12)	4(4)	4(4)	5(5)
ATLAS 7 TeV dileptonic 1607.07281	4	2(3)	1.9(1.9)	1.6(1.6)	1.1(1.1)
ATLAS 8 TeV dileptonic 1607.07281	5	0.2(0.2)	0.4(0.5)	0.4(0.4)	0.2(0.2)
ATLAS 7 TeV semileptonic 1407.0371	4	0.9(1.0)	5(6)	6(6)	3(3)
$\sigma(t\bar{t})$ all ATLAS + CMS incl. data	10	11(26)	16(61)	16(43)	11(12)
Total	122	101(117)	115(337)	113(262)	129(172)

- Global and partial χ^2 values for each data set
  - number of data points (n) obtained in m_t^{pole} extraction
  - different PDF sets ABMP16, CT18, MHST20, NNPDF4.0
- Additional χ^2 values in parentheses omit PDF uncertainties

Top-quark mass determination (II)

Garzelli. Mazzitelli. SM. Zenaiev '23

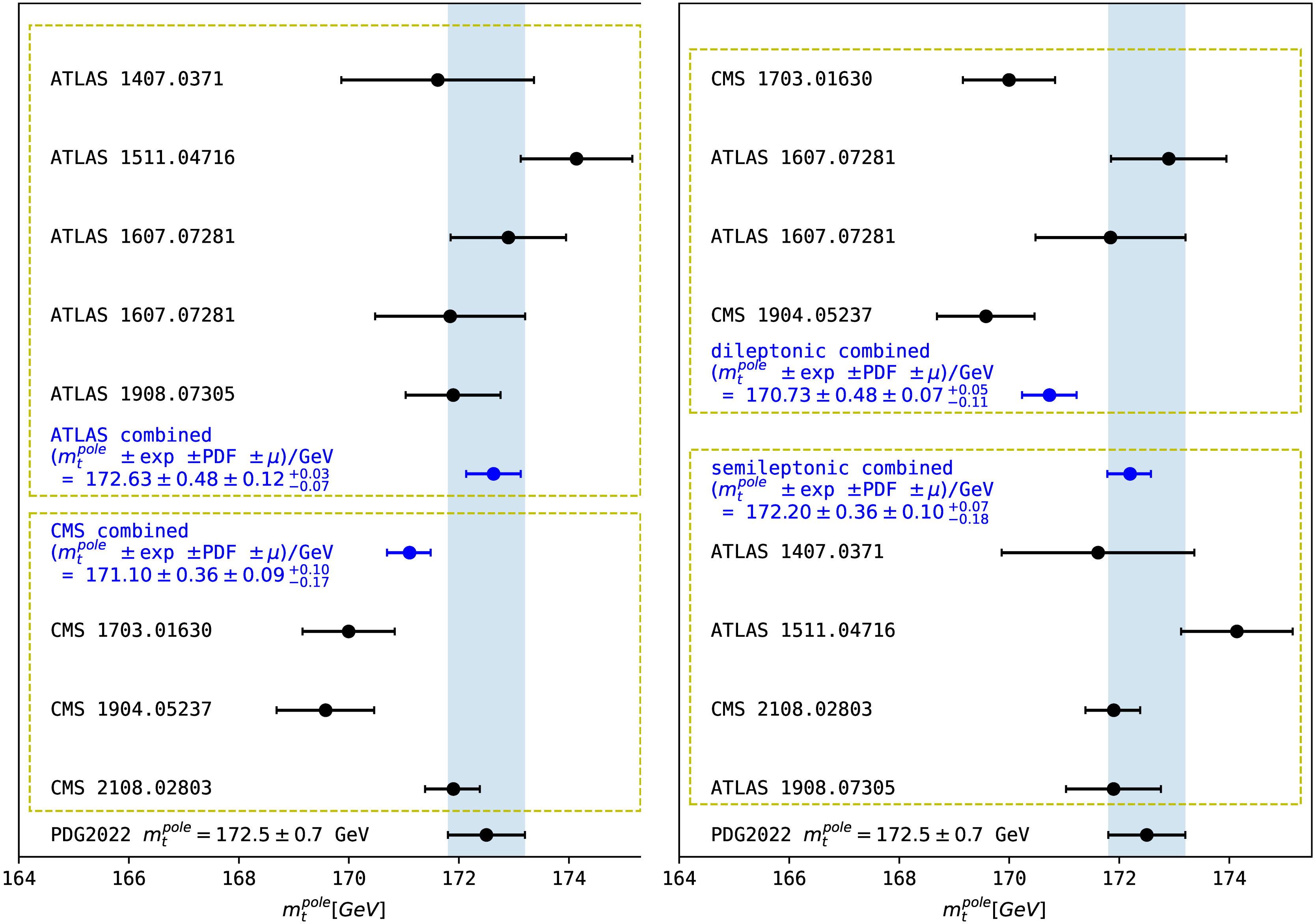

Fate of the Universe

- Condition of absolute stability of electroweak vacuum at Planck scale M_{Planck} requires Higgs self-coupling $\lambda(\mu_r) \geq 0$
  - correlation between Higgs mass m_H, m_t and $\alpha_s(M_Z)$ at $\mu = M_{\mathrm{Planck}}$

$$m_H \;\geq\; 129.6 + 2.0 \times \left(m_t^{\mathrm{pole}} - 173.34\ \mathrm{GeV} \right) - 0.5 \times \left(\frac{\alpha_s(M_Z) - 0.1184}{0.0007} \right) \pm 0.3\ \ \mathrm{GeV}$$

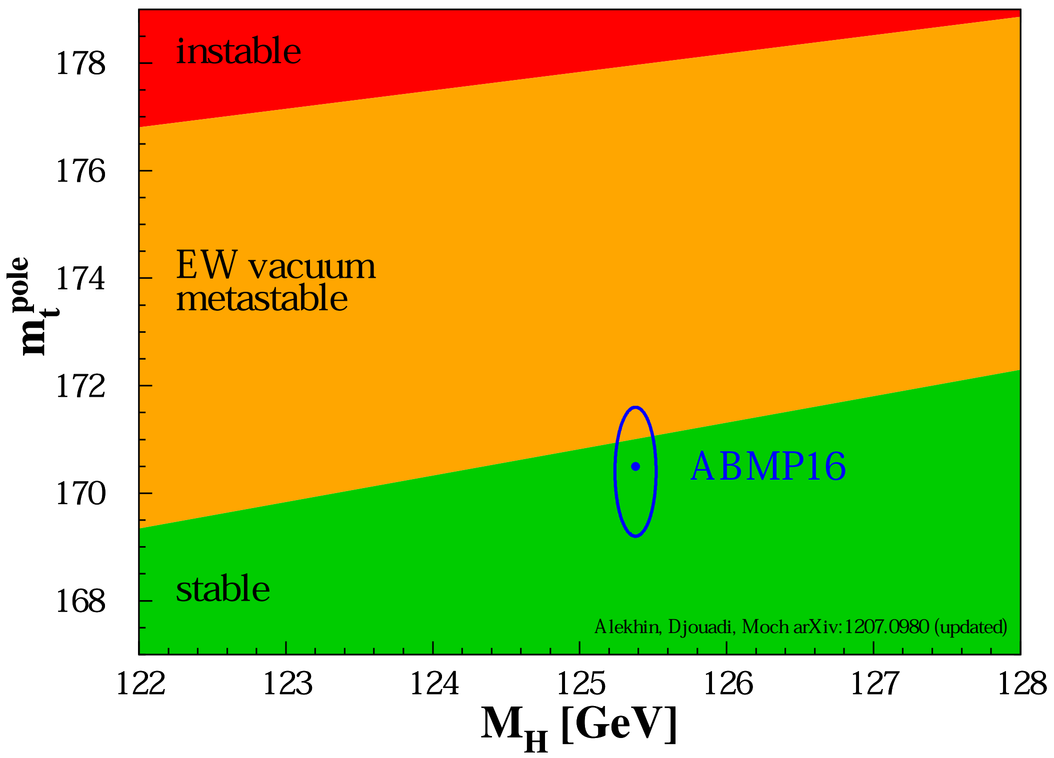

- NNLO analyses
  Bezrukov, Kalmykov, Kniehl, Shaposhnikov ‘12; Degrassi et al. ‘12; Buttazzo et al. ‘13; Bednyakov, Kniehl, Pikelner, Veretin ‘15

Drell-Yan process

Data in global PDF fits (II)

DY data in ABMP16 analysis

- High precision experimental data from LHC ATLAS, CMS, LHCb and Tevatron D0 useful for determinations of parton distributions
  - statistically significant $NDP = 172$ in ABMP16
- Differential distributions in decay lepton pseudo-rapidity extend kinematics to forward region
  - sensitivity to light quark flavors at $x \simeq 10^{-4}$
  - leading order kinematics with:

    $\sigma(W^+) \simeq u(x_2)\bar{d}(x_1)$ and $\sigma(W^-) \simeq d(x_2)\bar{u}(x_1)$;

    $\sigma(Z) \simeq Q_u^2 u(x_2)\bar{u}(x_1) + Q_d^2 d(x_2)\bar{d}(x_1)$
  - cf. DIS: $\sigma(\mathrm{DIS}) \simeq q_u^2 u(x) + q_d^2 d(x)$

Seaquest experiment

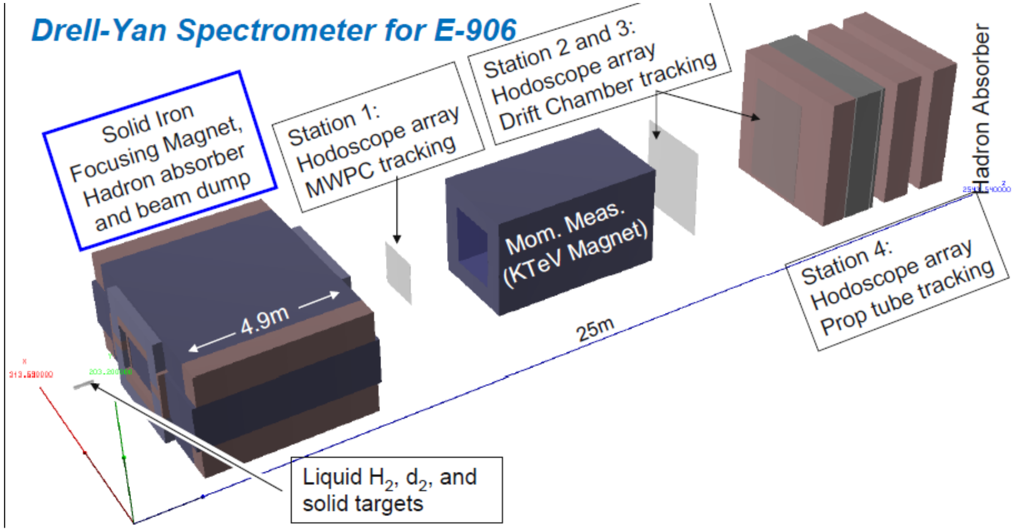

- Fermilab E-906/SeaQuest experiment is part of series of fixed target DY experiments
- Measurements of proton beam on deuterium target
- Invariant mass of observed γ^* decay products fixed to approximately $M_{\gamma^*} \sim 5$ GeV

Seaquest parton kinematics

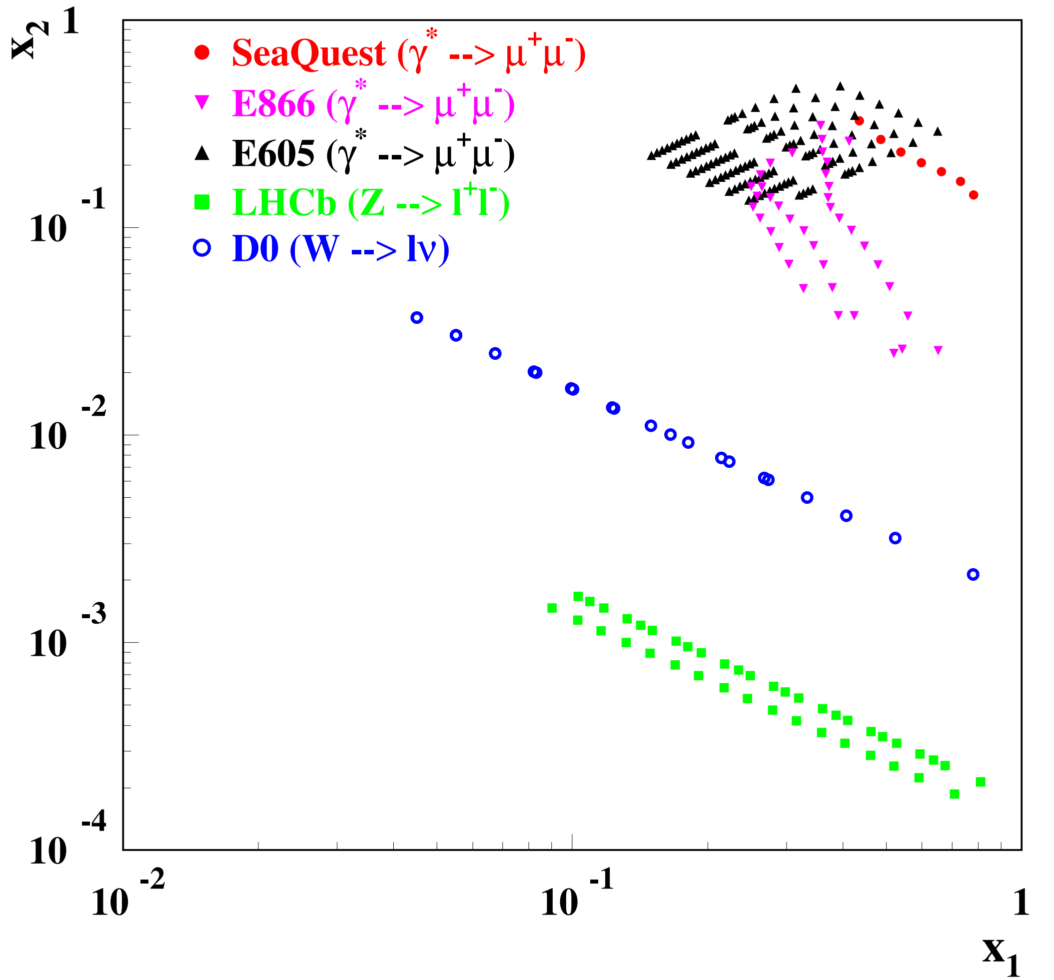

- Coverage of (x_1, x_2) plane by SeaQuest   Alekhin, Garzelli, Kulagin, S.M. ‘23
- DY data sets used in ABMP16 PDF fits extending to high (x)
  - Fermilab fixed-target experiment E866, E605
  - LHCb Z-boson rapidity distribution
  - D0 charged-lepton rapidity distribution

Light flavor PDFs from Seaquest data

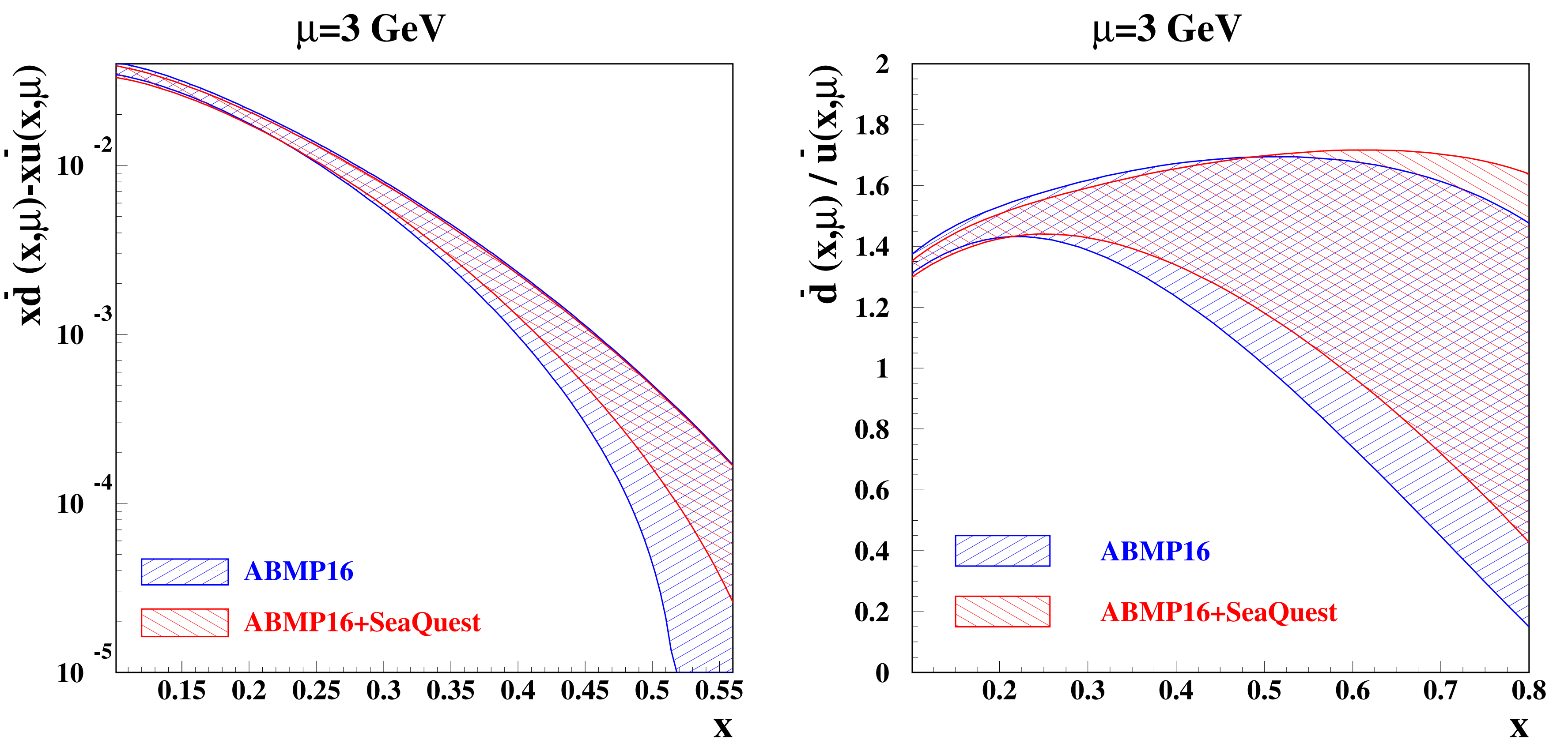

- 1σ bands for sea distributions in PDF fit with Seaquest data compared to ABMP16 fit Alekhin, Garzelli, Kulagin, S.M. '23
  - left: $n_f = 3$-flavor isospin asymmetry $x(\bar{d} - \bar{u})(x)$
  - right: ratio $\bar{d}/\bar{u}$ as a function of x

$\bar{d}/\bar{u}$ ratio from SeaQuest

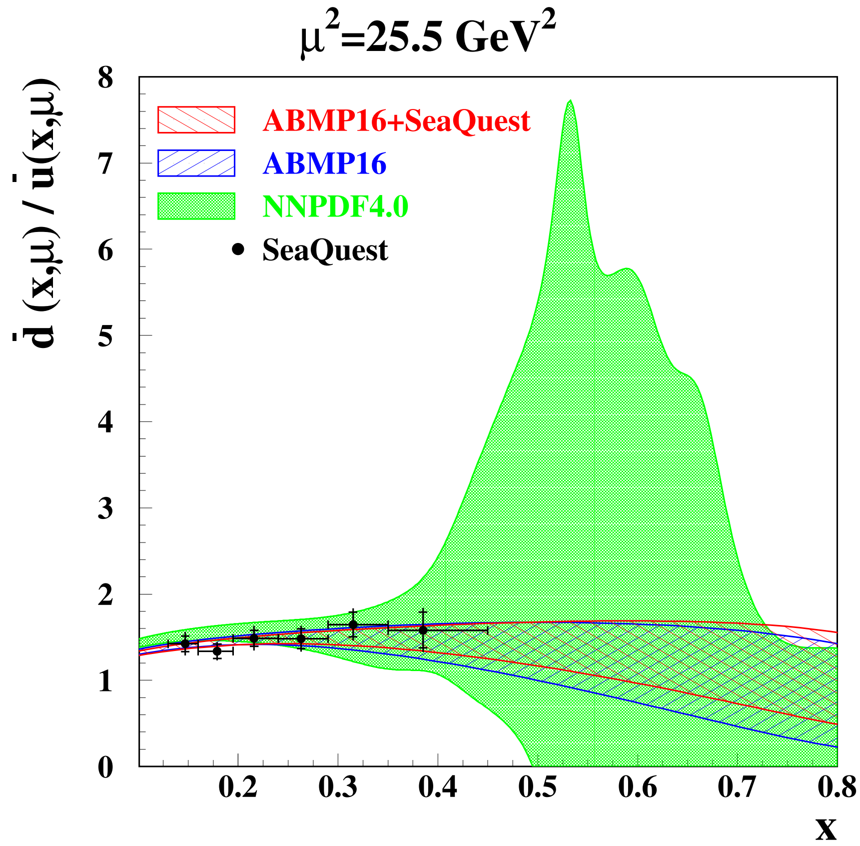

- 1σ bands for $\bar{d}/\bar{u}$ ratio at scale $\mu^2 = 25.5$ GeV^2 with comparison to SeaQuest extraction — Alekhin, Garzelli, Kulagin, S.M. '23
    - SeaQuest data has been included in NNPDF4.0 NNLO PDF fit

New physics searches

Searches at high scales

- Explore TeV region for deviations from Standard Model predictions
- Different theory approaches
  - parametrization of cross sections within the Standard Model as effective theory (SMEFT)

$$\mathcal{L} = \mathcal{L}^{(\mathrm{SM})} + \frac{1}{\Lambda^2} \sum_{j=1}^{N_6} C_j^{(6)} \, \mathcal{O}_j^{(6)} \;,$$

  - direct searches, e.g. new Z'-gauge boson
- Theory predictions depended on parton kinematics at high x
  - PDF uncertainty at high x can easily dominate overall error budget
  - estimates beyond measured kinematic range needed

Z-boson production at high invariant mass

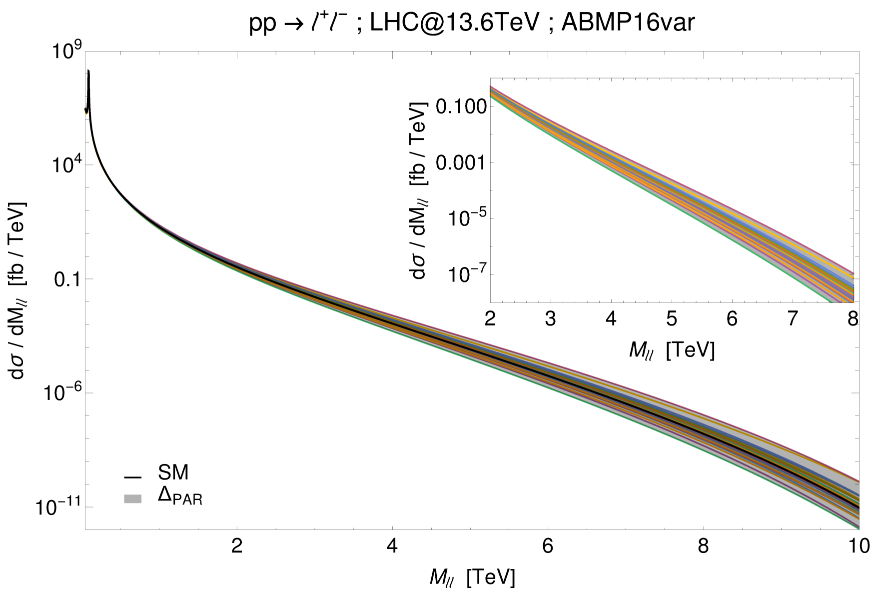

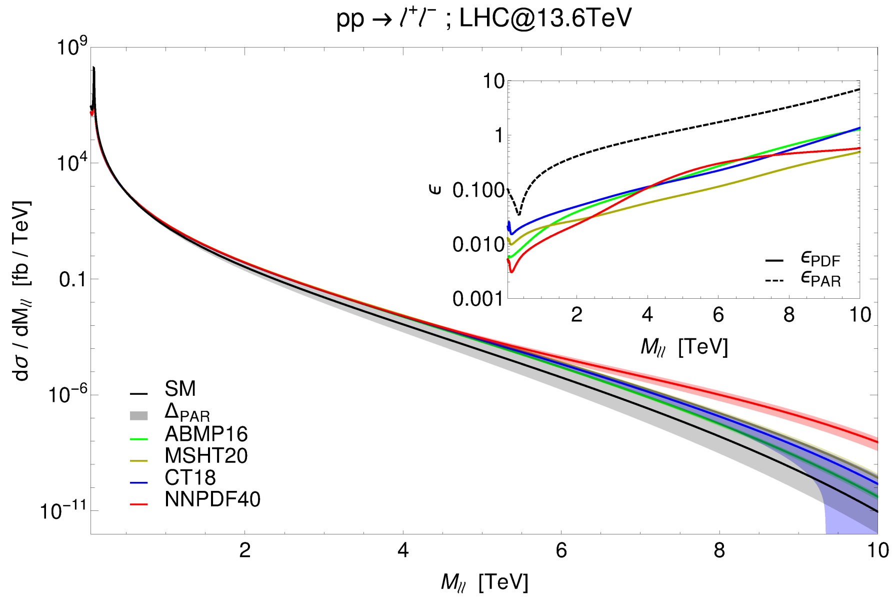

- ABMP16 NNLO PDFs, but large x part of u and d modified

  Fiaschi, Giuli, Hautmann, S.M., Moretti '22

  - parametrization $\sim (1-x)^b$ with variation of exponent $b \pm 0.3$ and 0.5 (recall $b \sim 3 \dots 8$) $\longrightarrow$ ABMP16var
  - keep vanishing $\bar{d}/\bar{u}$ as $x \to 1$
- Differential cross section for Z-boson production in M_{ll} at LHC with $\sqrt{s}$ = 13.6 TeV
  - left: results for all ABMP16var members
  - right: comparison with results from standard PDF sets

Predictions for models with Z'-boson

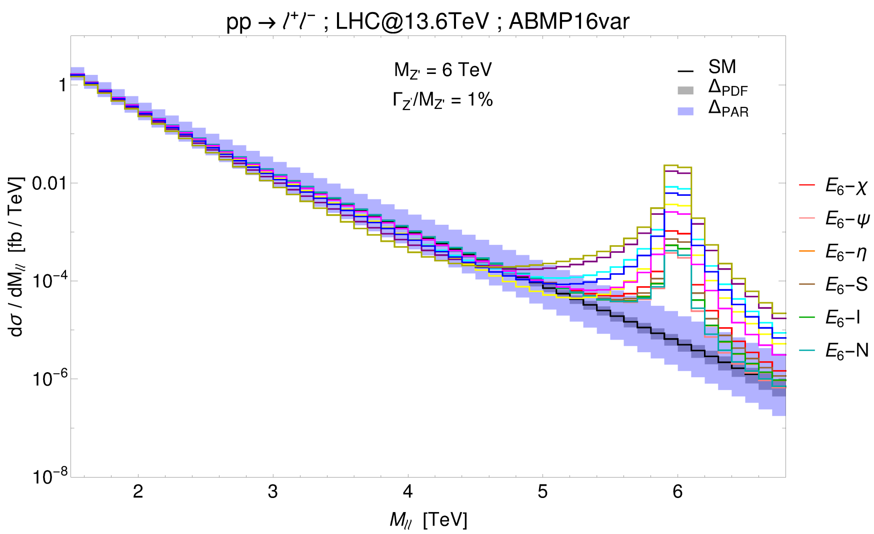

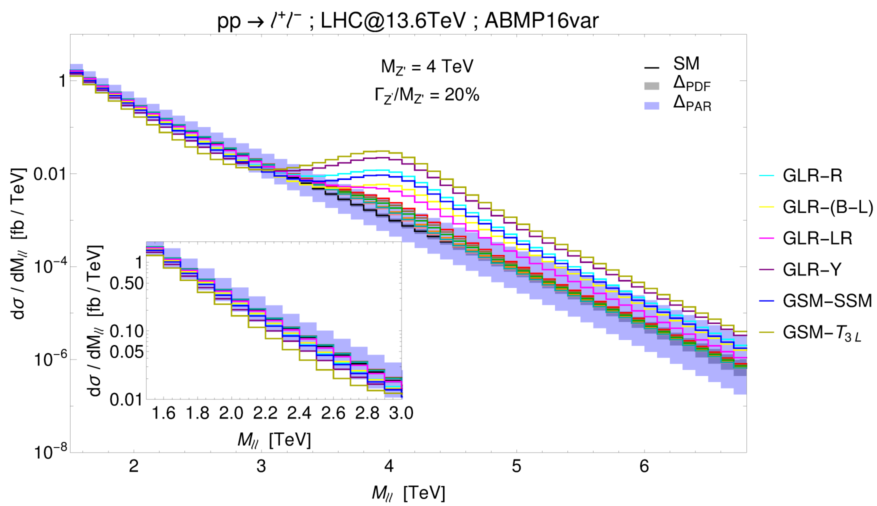

- Differential cross section in M_{ll} at LHC with $\sqrt{s}$ = 13.6 TeV for a series of single Z' benchmark models using ABMP16var PDFs

  Fiaschi, Giuli, Hautmann, S.M., Moretti '22

  - left: results for $M_{Z'} = 6$ TeV, $\Gamma_{Z'}/M_{Z'} = 1\%$
  - right:results for $M_{Z'} = 4$ TeV, $\Gamma_{Z'}/M_{Z'} = 20\%$

Forward-backward asymmetry

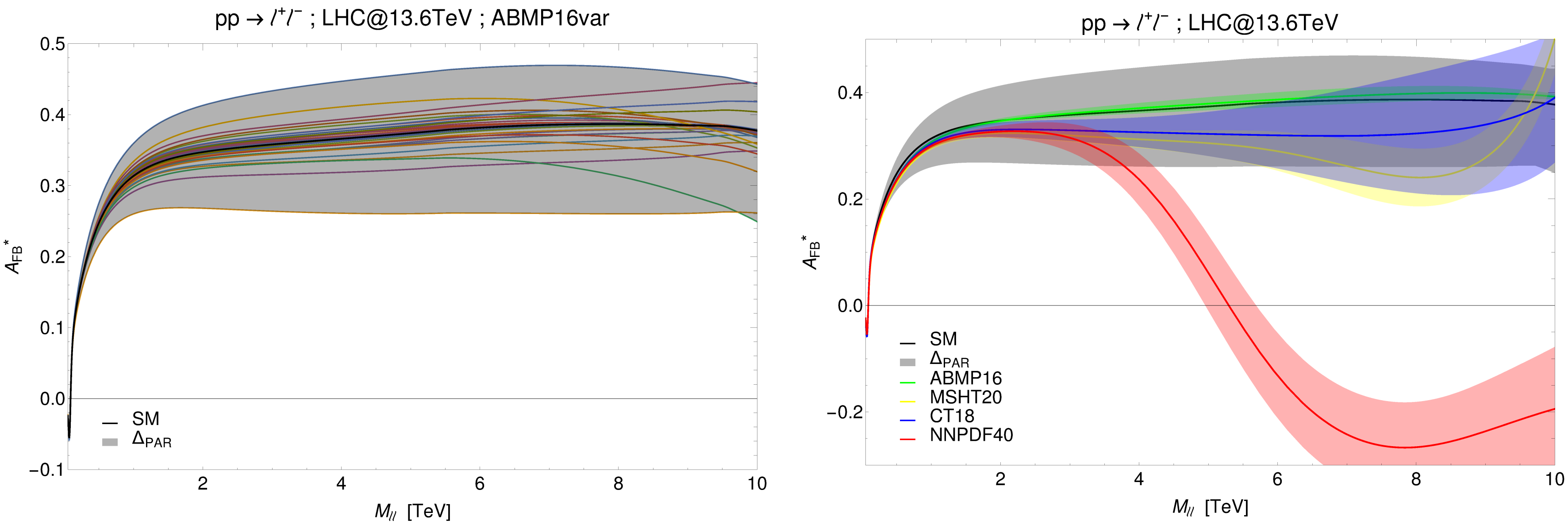

- Forward-backward asymmetry $A^*_{\rm FB}$

$$A^*_{\rm FB} = \frac{d\sigma/(dM_{\ell\ell}dy_{\ell\ell})[\cos\theta^* > 0] - d\sigma/(dM_{\ell\ell}dy_{\ell\ell})[\cos\theta^* < 0]}{d\sigma/(dM_{\ell\ell}dy_{\ell\ell})[\cos\theta^* > 0] + d\sigma/(dM_{\ell\ell}dy_{\ell\ell})[\cos\theta^* < 0]}.$$

- Asymmetry $A^*_{\rm FB}$ in M_{ll} at LHC with $\sqrt{s}$ = 13.6 TeV

  Fiaschi, Giuli, Hautmann, S.M., Moretti '22

  - left: results for all ABMP16var members
  - right: comparison with results from standard PDF sets

Predictions for models with Z'-boson

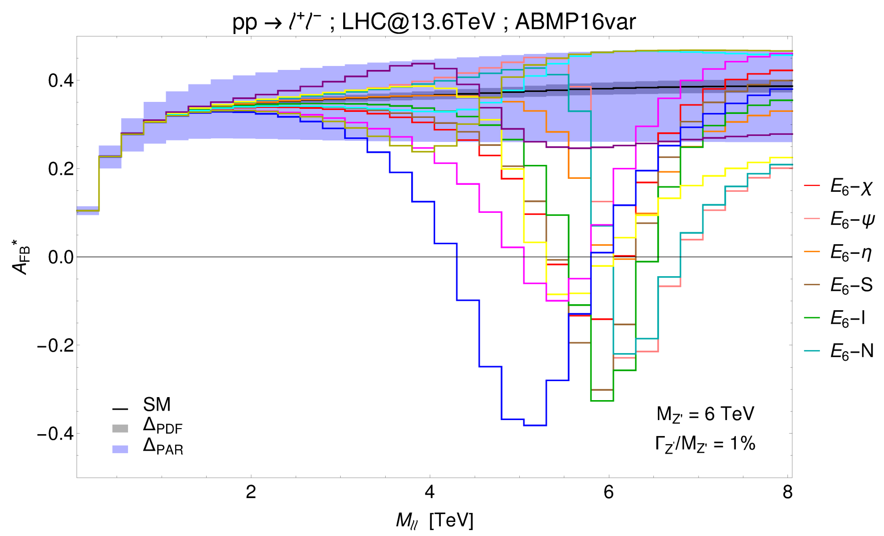

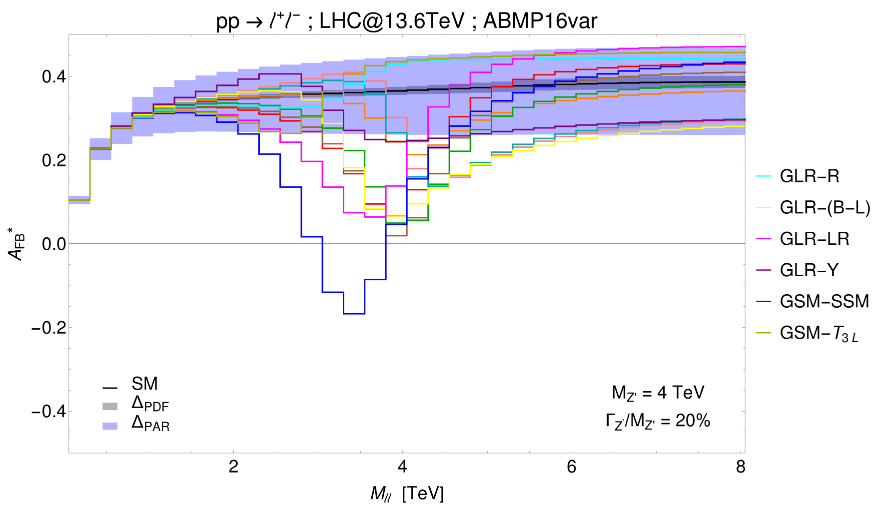

- Asymmetry $A^*_{\rm FB}$ in M_{ll} at LHC with $\sqrt{s}$ = 13.6 TeV for a series of single Z' benchmark models using ABMP16var PDFs

  Fiaschi, Giuli, Hautmann, S.M., Moretti '22

  - left: results for $M_{Z'} = 6$ TeV, $\Gamma_{Z'}/M_{Z'} = 1\%$
  - right:results for $M_{Z'} = 4$ TeV, $\Gamma_{Z'}/M_{Z'} = 20\%$

$A^*_{\rm FB}$ *at high invariant mass*

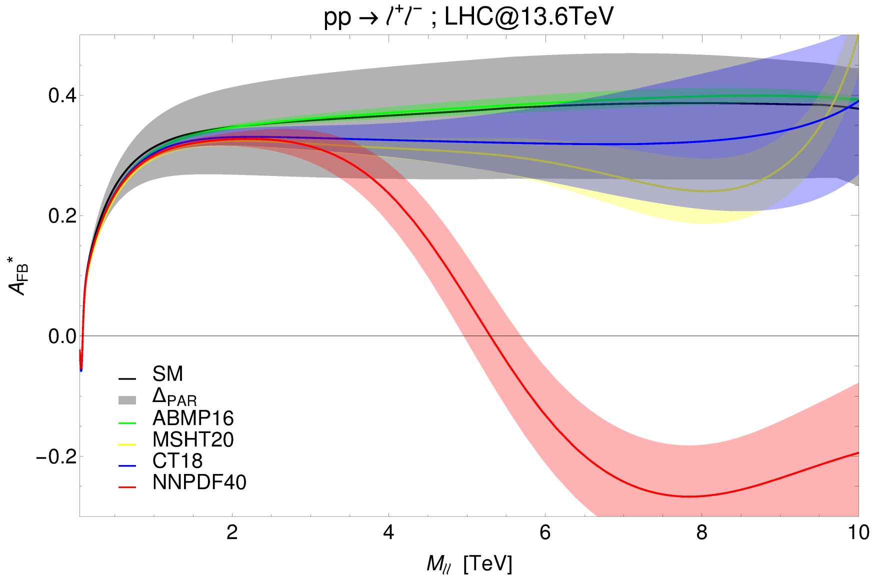

- Explaining the $A^*_{\rm FB}$ prediction by NNPDF4.0
- Recall leading order kinematics $\sigma(Z) \simeq Q_u^2 u(x_2)\bar{u}(x_1) + Q_d^2 d(x_2)\bar{d}(x_1)$
- Define slope of light quark PDFs $f_q(x,\mu^2) \sim (1-x)^{b_q}$

$$\beta_q(x) = \frac{\partial |x f_q(x,\mu^2)|}{\partial \ln(1-x)}$$

  - positive A_{FB} require light flavor sea PDFs ($\bar{u}$ and $\bar{d}$) to fall off faster at large-x than valence quarks (u and d)
  - $\beta_{\bar{u}}(x) > \beta_u(x)$ and $\beta_{\bar{d}}(x) > \beta_d(x)$ for all values of x

Summary

- Experimental precision of $\lesssim 1\%$ makes theoretical predictions at NNLO in QCD mandatory
  - theoretical predictions at NNLO in QCD nowadays standard
- Need public NNLO QCD codes for Standard Model processes in hadro-production (incl. benchmarking)
- Precision studies of hadron structure
  - dedicated analysis of experimental data
  - correlations of PDFs with $\alpha_s(M_Z)$ and top-quark mass extraction
- DY data from LHC and from fixed target experiments allow for good control of light flavor content in proton at high x
- High x parton kinematics is important region for new physics searches
  - A_{FB} for Z-boson in the TeV range

Future tasks

- Joint effort theory and experiment